Improved Referencing Schemes for 2.5D Wave Field Synthesis Driving Functions

Gergely Firtha, Péter Fiala, Frank Schultz, and Sascha Spors, *Member, IEEE*

***Abstract*—Wave Field Synthesis allows the reconstruction of an arbitrary target sound field within a listening area by using a secondary source contour of spherical monopoles. While phase correct synthesis is ensured over the whole listening area, amplitude deviations are present besides a predefined reference curve. So far, the existence and potential shapes of this reference curve was not extensively discussed in the Wave Field Synthesis literature. This paper introduces improved driving functions for 2.5D Wave Field Synthesis. The novel driving functions allow for the control of the locations of amplitude correct synthesis for arbitrarily shaped—possibly curved—secondary source distributions. This is achieved by deriving an expressive physical interpretation of the stationary phase approximation leading to the presented unified Wave Field Synthesis framework. The improved solutions are better suited for practical applications. Additionally, a consistent classification of existing implicit and explicit 2.5D sound field synthesis solutions as special cases of the unified framework is given.**

***Index Terms*—Local wavenumber vector, stationary phase approximation, wave field synthesis, 2.5D WFS.**

I. Introduction

WAVE Field Synthesis (WFS) [1]–[4] is a well established sound field synthesis (SFS) technique for the reproduction of an arbitrary target sound field over a listening area. Synthesis is performed using a loudspeaker array, termed as the secondary source distribution (SSD). The objective of WFS is to find the appropriate input signals for the SSD—termed as the driving functions—so that the resultant sound field coincides with the target sound field at each point of the listening area.

WFS originates from the boundary integral representation of the target sound field [5]–[7] in a synthesis domain bounded by a smooth SSD surface. The Kirchhoff–Helmholtz integral representation of the target field implicitly contains the appropriate WFS driving functions. However, 3D surface SSDs are impractical to implement, and 2D SSD contours are realized instead. This dimensionality reduction has two important consequences. Phase correct synthesis is restricted to a 2D synthesis plane bounded by the SSD contour, and the synthesized field cannot be amplitude correct in the whole synthesis area, only at specific reference locations.

This article focuses on WFS referencing, i.e., the analysis and control of positions where the synthesized field is amplitude correct.

During the last three decades two main WFS methodologies have been developed, commonly referred to as *traditional WFS* and *revisited WFS*. The two approaches mainly differ in the way of the dimensionality reduction and have different referencing limitations.

Traditional WFS aims to synthesize a virtual point source using a 2D linear contour of secondary point sources. The method applies the 3D Rayleigh integral to the virtual point source field [8]–[11], and dimensionality reduction is performed by means of the stationary phase approximation (SPA) of rapidly oscillating integrals. The resulting so-called 2.5D Neumann Rayleigh integral [3] contains the appropriate driving functions. Note that the very initial derivation [1], [2] led to the 2.5D Dirichlet Rayleigh integral using a SSD containing secondary dipole sources, instead of spherical monopoles.

Revisited WFS [12]–[14] can be used to synthesize a 2D virtual sound field with a 2D contour of secondary point sources. This approach stems from the 2D Neumann Rayleigh integral that assumes 2D secondary line sources. In order to obtain driving functions for secondary point sources instead of line sources, the SPA is applied to the 2D Rayleigh integral. As 3D virtual fields are not unambiguously given on the SSD contour, revisited WFS theory is unable to synthesize 3D virtual fields.

Theoretically, both WFS approaches are able to reconstruct the phase—i.e. the wavefront shape—of the virtual sound field over the listening area. However, due to different formulations of the dimensionality reduction, the approaches exhibit different amplitude deviations. The traditional WFS theory references the amplitude of the virtual point source typically to a reference line parallel to the SSD. The revisited WFS theory optimizes amplitude correct synthesis in a single reference point in the synthesis domain. This, as a side effect, results in amplitude correct synthesis along a reference curve which depends on the virtual source field. The exact *positions of amplitude correct synthesis* (PCS) in the revisited WFS theory have not been investigated in detail so far.

In the present treatise we derive a unified WFS framework allowing the synthesis of arbitrary 2D and 3D virtual sound fields using a 2D SSD contour of point sources. The unified framework allows to optimize amplitude correct synthesis to an arbi-

Manuscript received August 1, 2016; revised January 14, 2017 and March 20, 2017; accepted March 26, 2017. Date of publication March 29, 2017; date of current version April 24, 2017. The associate editor coordinating the review of this manuscript and approving it for publication was Prof. Augusto Sarti. *(Corresponding author: Gergely Firtha.)*

G. Firtha and P. Fiala are with the Department of Networked Systems and Services, Budapest University of Technology and Economics, Budapest 1117, Hungary (e-mail: firtha@hit.bme.hu; fiala@hit.bme.hu).

F. Schultz is with the Audio Communication Group, Technische Universität Berlin, Berlin 10623, Germany (e-mail: franks.schultz@tu-berlin.de).

S. Spors is with the Institute of Communications Engineering, Universität Rostock, Rostock 18119, Germany (e-mail: sascha.spors@uni-rostock.de).

Color versions of one or more of the figures in this paper are available online at http://ieeexplore.ieee.org.

Digital Object Identifier 10.1109/TASLP.2017.2689245

trarily chosen reference curve. This is achieved by introducing a physical interpretation for the SPA, using the local wavenumber vector concept. Besides the theoretical extension of the general WFS theory, the presented framework allows the practical control of amplitude and phase correct synthesis over the listening area, using an arbitrarily shaped loudspeaker ensemble.

The article is structured as follows: Section II provides a brief overview on the existing WFS techniques, their involved SPAs and limitations. As the main theoretical contribution, Section III presents the physical interpretation of the SPA and proposes improved WFS driving functions by introducing the so-called referencing function. Section IV applies the unified WFS methodology for 2D and 3D sound fields and various practical referencing approaches. It is shown, how the reference curve can be controlled by defining the corresponding referencing function. Furthermore, the connections of the presented unified framework with the previous WFS approaches are highlighted. Finally, in Section V it is demonstrated, that the new approach precisely holds for non-linear SSD contours as well. This allows for convenient and practically relevant implementation of the new driving functions when using arbitrarily shaped SSD contours.

II. Theoretical Background

This section provides an overview on the existing WFS approaches. In general, to implicitly derive 2.5D SFS driving functions from either the 3D or the 2D Neumann Rayleigh integral the SPA is applied for. Therefore, this integral approximation is briefly revisited initially.

A. Stationary Phase Approximation (SPA)

The SPA [15]–[17] yields an approximate expression for integrals of the form (with $\mathrm{j}^2 = -1$, $F(z) \in \mathbb{R}$, $\phi(z) \in \mathbb{R}$)

$$I = \int_{-\infty}^{\infty} F(z)\, \mathrm{e}^{\mathrm{j}\phi(z)}\, \mathrm{d}z, \tag{1}$$

where $\mathrm{e}^{\mathrm{j}\phi(z)}$ is rapidly oscillating and $F(z)$ is comparably slowly varying. The method relies on the second order truncated Taylor series of the exponent around the stationary point z^*, where $\phi'_z(z^*) = 0$ and $\phi''_{zz}(z^*) \neq 0$, with ϕ'_z denoting the derivative w.r.t. z. Supposing that $F(z)$ is slowly varying, it is assumed, that the integral of rapid oscillation cancels out, and the largest contribution to the total integral arises from the immediate surroundings of the stationary point. The approximate expression of the integral becomes [15, (2.7.18)]

$$\begin{aligned} I &\approx F(z^*)\, \mathrm{e}^{+\mathrm{j}\phi(z^*)} \int_{-\infty}^{\infty} \mathrm{e}^{+\mathrm{j}\frac{1}{2}\phi''_{zz}(z^*)(z-z^*)^2}\, \mathrm{d}z \\ &= \sqrt{\frac{2\pi}{|\phi''_{zz}(z^*)|}}\, F(z^*)\, \mathrm{e}^{+\mathrm{j}\phi(z^*)+\mathrm{j}\frac{\pi}{4}\,\mathrm{sgn}(\phi''_{zz}(z^*))}. \end{aligned} \tag{2}$$

B. 3D and 2D Neumann Rayleigh Integrals

The starting point of WFS theory is the Rayleigh integral formulation of an arbitrary sound field given on an infinite plane. For the sake of convenience the $x-z$-plane is chosen with positions $\mathbf{x}_0 = [x_0,\ 0,\ z_0]^{\mathrm{T}}$. At an arbitrary (receiver/listener) position $\mathbf{x} = [x,\ y > 0,\ z]^{\mathrm{T}}$ the 3D Neumann Rayleigh integral [18, Ch. 23.5] reads

$$P(\mathbf{x},\omega) = -2 \iint_{-\infty}^{\infty} \left.\frac{\partial P(\mathbf{x},\omega)}{\partial y}\right|_{\mathbf{x}=\mathbf{x}_0} G_{3\mathrm{D}}(\mathbf{x}-\mathbf{x}_0,\omega)\, \mathrm{d}z_0\, \mathrm{d}x_0, \tag{3}$$

with the 3D freefield Green's function (i.e. the field of the ideal point source) given as [18, Ch. 27]

$$G_{3\mathrm{D}}(\mathbf{x}-\mathbf{x}_0,\omega) = \frac{1}{4\pi} \frac{\mathrm{e}^{-\mathrm{j}k|\mathbf{x}-\mathbf{x}_0|}}{|\mathbf{x}-\mathbf{x}_0|}, \tag{4}$$

where $k = \frac{\omega}{c}$ denotes the wave number, c defines the speed of sound, and the $\mathrm{e}^{+\mathrm{j}\omega t}$ time convention is applied.

Assuming a 2D sound field independent from the z-coordinate, the field at $y > 0$ can be given by the 2D Neumann Rayleigh integral [3], [12]:

$$\begin{aligned} P(\mathbf{x},\omega) = \ & -2 \int_{-\infty}^{\infty} \left.\frac{\partial P(\mathbf{x},\omega)}{\partial y}\right|_{\mathbf{x}=\mathbf{x}_0} \\ & \underbrace{\int_{-\infty}^{\infty} G_{3\mathrm{D}}(\mathbf{x}-\mathbf{x}_0,\omega)\, \mathrm{d}z_0}_{G_{2\mathrm{D}}(\mathbf{x}-\mathbf{x}_0,\omega)}\, \mathrm{d}x_0 \end{aligned} \tag{5}$$

with the 2D freefield Green's function (i.e. the field of the ideal line source) given as [18, Ch. 27]

$$G_{2\mathrm{D}}(\mathbf{x}-\mathbf{x}_0,\omega) = -\frac{\mathrm{j}}{4} H_0^{(2)}\left(k|\mathbf{x}-\mathbf{x}_0|\right), \tag{6}$$

where $H_\nu^{(2)}(\cdot)$ denotes the Hankel function of the second kind and ν-th order [19, Ch. 10].

Integral (5) represents SFS by applying a linear distribution of vertical line sources along the x-axis, whereas (3) describes SFS applying an infinite planar 3D point source distribution.

Both (3) and (5) are special cases of the general Kirchhoff-Helmholtz boundary integral formulation of the virtual field. These Neumann Rayleigh representations are obtained by eliminating the practically hardly realizable dipole secondary sources by the assumption of planar/linear SSDs [11].

C. Revisited 2.5D WFS Theory

The revisited WFS theory [12] starts out from the 2D Rayleigh integral (5). As a consequence, this approach restricts the synthesis to 2D virtual sound fields. For points in the far field within the synthesis plane (i.e. $z = 0$), the vertical integral of the Green's function in (5) may be approximated asymptotically using the SPA with the stationary position $z_0^* = 0$. The approximation yields the 2.5D Neumann Rayleigh integral for a 2D sound field

$$\begin{aligned} P(\mathbf{x},\omega) = \ & -2 \int_{-\infty}^{\infty} \left.\frac{\partial P(\mathbf{x},\omega)}{\partial y}\right|_{\mathbf{x}=\mathbf{x}_0} \\ & \cdot \left[\sqrt{\frac{2\pi|\mathbf{x}-\mathbf{x}_0|}{\mathrm{j}k}}\, G_{3\mathrm{D}}(\mathbf{x}-\mathbf{x}_0,\omega)\right] \mathrm{d}x_0, \end{aligned} \tag{7}$$

with $\mathbf{x} = [x,\ y > 0,\ 0]^{\mathrm{T}}$ and $\mathbf{x}_0 = [x_0,\ 0,\ 0]^{\mathrm{T}}$. The 2.5D formulation applies a linear distribution of point sources along the

x-axis, which can be practically approximated with closed box loudspeakers arranged along a horizontal contour. The discrepancy between the 2D and the 3D Green's function is referred to as *secondary source dimensionality mismatch*, which is compensated regarding both the frequency response and the attenuation factor by $\sqrt{\frac{2\pi|\mathbf{x}-\mathbf{x}_0|}{\mathrm{j}k}}$, cf. [12, (24)].

The implicitly contained driving function $D(x_0,\omega)$ for a 2D virtual field is [12, (26)]

$$D(x_0,\omega) = -2\sqrt{\frac{2\,\pi}{\mathrm{j}k}}\sqrt{|\mathbf{x}-\mathbf{x}_0|}\;\left.\frac{\partial P(\mathbf{x},\omega)}{\partial y}\right|_{\mathbf{x}=\mathbf{x}_0}. \tag{8}$$

This driving function ensures amplitude correct synthesis at the receiver location $\mathbf{x}$. In order to obtain driving functions independent of the receiver location, either $\mathbf{x}$ is fixed to a designated reference point $\mathbf{x}_{\mathrm{ref}}$ [12], or the entire correction factor $|\mathbf{x}-\mathbf{x}_0|$ is set to a constant value d_{ref} [14].

It is worth noting that no 3D virtual sound field can be synthesized by (5). Even by applying ideal line sources, the correct synthesis of a point source is impossible since amplitude errors would be present in the synthesized field. This phenomenon is referred to as *virtual source dimensionality mismatch*, and has to be accounted for when aiming for a 3D virtual sound field. In [20] an alternative method—called primary source correction—was proposed to compensate for this virtual source dimensionality mismatch for a single receiver position.

D. Traditional 2.5D WFS Theory

Traditional WFS, e.g. [9] utilizes the 3D Rayleigh integral (3), and assumes a virtual point source (4) located in $\mathbf{x}_{\mathrm{s}} = [x_s,\, y_s < 0,\, 0]^{\mathrm{T}}$. By using the high-frequency gradient approximation (18) of the virtual field's y-derivative on the Rayleigh plane (refer to [11, Ch. 2.3]), the Rayleigh integral reads

$$P(\mathbf{x},\omega) = -2\iint_{-\infty}^{\infty}\frac{\mathrm{j}\,k\,y_s}{4\pi}\frac{\mathrm{e}^{-\mathrm{j}k|\mathbf{x}_0-\mathbf{x}_s|}}{|\mathbf{x}_0-\mathbf{x}_s|^2}\frac{1}{4\pi}\frac{\mathrm{e}^{-\mathrm{j}k|\mathbf{x}-\mathbf{x}_0|}}{|\mathbf{x}-\mathbf{x}_0|}\,\mathrm{d}z_0\,\mathrm{d}x_0. \tag{9}$$

Approximating the vertical (inner) integral by the SPA around $z_0^* = z_0 = 0$, the $\sqrt{\ }$-factor in (2) results in

$$\sqrt{\frac{2\pi}{|\phi''_{zz}(z_0^*)|}} = \sqrt{\frac{2\pi}{k}}\sqrt{\frac{|\mathbf{x}_0-\mathbf{x}_s|\cdot|\mathbf{x}-\mathbf{x}_0|}{|\mathbf{x}_0-\mathbf{x}_s|+|\mathbf{x}-\mathbf{x}_0|}} \tag{10}$$

now with $\mathbf{x} = [x,\, y>0,\, 0]^{\mathrm{T}}$, $\mathbf{x}_0 = [x_0,\, 0,\, 0]^{\mathrm{T}}$.

Note the difference of $|\phi''_{zz}(z_0^*)| = \frac{k}{|\mathbf{x}-\mathbf{x}_0|}$ for a 2D virtual field (7) and $|\phi''_{zz}(z_0^*)| = \frac{k}{|\mathbf{x}-\mathbf{x}_0|} + \frac{k}{|\mathbf{x}_0-\mathbf{x}_s|}$ for the virtual point source. In the latter case, not only the secondary source, but also the virtual source attenuation is corrected.

The vertical SPA of (9) yields the 2.5D Neumann Rayleigh integral for a virtual point source

$$P(\mathbf{x},\omega) = -2\int_{-\infty}^{\infty}\sqrt{\frac{2\pi}{\mathrm{j}k}}\sqrt{\frac{|\mathbf{x}_0-\mathbf{x}_s|\cdot|\mathbf{x}-\mathbf{x}_0|}{|\mathbf{x}_0-\mathbf{x}_s|+|\mathbf{x}-\mathbf{x}_0|}} \cdot \left.\frac{\partial\, G_{3\mathrm{D}}(\mathbf{x}-\mathbf{x}_s,\omega)}{\partial y}\right|_{\mathbf{x}=\mathbf{x}_0} G_{3\mathrm{D}}(\mathbf{x}-\mathbf{x}_0,\omega)\,\mathrm{d}x_0. \tag{11}$$

It implicitly contains the driving function, consisting of the following terms

$$D(x_0,\omega) = \underbrace{\sqrt{\frac{2\pi}{\mathrm{j}k}}}_{\text{SSD freq.compensation}}\quad\underbrace{\sqrt{|\mathbf{x}-\mathbf{x}_0|}}_{\text{SSD amp.compensation}} \underbrace{\sqrt{\frac{|\mathbf{x}_0-\mathbf{x}_s|}{|\mathbf{x}_0-\mathbf{x}_s|+|\mathbf{x}-\mathbf{x}_0|}}}_{\substack{\text{Virt. source}\\ \text{amp. comp.}}} \cdot \underbrace{-2\left.\frac{\partial P(\mathbf{x},\omega)}{\partial y}\right|_{\mathbf{x}=\mathbf{x}_0}}_{\text{2D driving function, HF approx.}} \tag{12}$$

Comparing this result with (8) it is revealed, that the virtual source mismatch can be compensated by the correction factor $\sqrt{\frac{|\mathbf{x}_0-\mathbf{x}_s|}{|\mathbf{x}_0-\mathbf{x}_s|+|\mathbf{x}-\mathbf{x}_0|}}$. The numerator stands for the attenuation correction from the virtual point source to the SSD, and the denominator for the correction from the virtual point source to the receiver position.

Similar to the revisited WFS case, this 2.5D driving function is receiver position dependent. As proven in e.g. [10, Ch. 3.1], by fixing the receiver position's y-coordinate to a constant value $y_{\mathrm{ref}} > 0$ and performing a second, horizontal SPA to the 2.5D Rayleigh integral (11), the compensation factor simplifies to

$$\frac{|\mathbf{x}-\mathbf{x}_0|}{|\mathbf{x}_0-\mathbf{x}_s|+|\mathbf{x}-\mathbf{x}_0|} = \frac{y_{\mathrm{ref}}}{y_{\mathrm{ref}}-y_s} \tag{13}$$

around the stationary point. Substituting into (12) yields the traditional 2.5D WFS driving function of the virtual point source (43) derived in IV-B2. In [10] it was furthermore discussed, that positions $\mathbf{x}(\mathbf{x}_0)$ might be chosen along the vector $\mathbf{x}_o - \mathbf{x}_s$ to obtain arbitrarily shaped reference curves, cf. [10, (3.30)]. This approach becomes proven and generalized within this article.

E. Limitations of the Existing WFS Approaches

Based on the foregoing, the limitations of the outlined WFS approaches can be concluded as follows:

1) Traditional WFS exclusively allows the synthesis of (optionally directional) point sources [8], [11], with amplitude correct synthesis restricted to a reference curve; widely spread a parallel line to a linear SSD [10].
2) The revisited WFS formulation allows the incorporation of arbitrary virtual source models, but ignores the virtual source dimensionality mismatch in case of a 3D virtual sound field. Furthermore, the target field's amplitude is optimized to a single reference point, and the resulting locations of amplitude correct synthesis have not been investigated so far.

In the following section a unified WFS formulation is introduced that overcomes the mentioned shortcomings. The application of this framework allows both the analysis of revisited and traditional WFS formulations as well as the derivation of driving functions with an arbitrarily chosen reference curve at which amplitude correct synthesis is ensured.

Note that the terminology *amplitude correct synthesis* may be misleading. Due to the several approximations introduced, no position of amplitude correct synthesis exists: both, the vertical and the horizontal SPA along with the high-frequency

gradient approximation assume high-frequency conditions. Positions of amplitude correct synthesis refer to locations where the synthesis is optimized within the validity of the stationary phase method.

III. Unified WFS Theory

This section presents the unified WFS framework. First, the local wavenumber vector concept is introduced, allowing a physical interpretation of the SPA applied to the Rayleigh integral. This is followed by introducing generalized WFS driving functions, with the possibility of optimizing amplitude correct synthesis on an arbitrary receiver curve within the synthesis plane.

A. Local Wavenumber Vector and SPA Interpretation

Consider an arbitrary steady state sound field represented in polar form with $A_P, \phi_P \in \mathbb{R}$

$$P(x,y,\omega) = A_P(x,y,\omega)\,\mathrm{e}^{\mathrm{j}\phi_P(x,y,\omega)}. \tag{14}$$

The dynamics of wave propagation is determined by the phase function $\phi_P(x,y,\omega)$: in the space-frequency domain the propagation direction/wave number vector of a sound field is given by the direction of maximum phase advance, i.e. the gradient of the phase of the sound field. For an arbitrary—for the sake of simplicity—propagating 2D sound field $P(x,y,\omega)$, the local wave number vector at an arbitrary point is given by

$$\mathbf{k}_P(x,y) = \begin{bmatrix} k_x(x,y) \\ k_y(x,y) \end{bmatrix} = -\nabla\phi_P(\mathbf{x},\omega) = -\begin{bmatrix} \dfrac{\partial}{\partial x} \\ \dfrac{\partial}{\partial y} \end{bmatrix} \phi_P(\mathbf{x},\omega). \tag{15}$$

The temporal frequency dependency of the wavenumber vector is omitted for the sake of brevity. This vector is perpendicular to the wavefront in each position. Since a 2D sound field, along with the dispersion relation $\left(\frac{\omega}{c}\right)^2 = k_x^2 + k_y^2$, is considered, the horizontal component k_x completely determines the direction of wave propagation for a given temporal frequency.

When the SPA is applied to the Rayleigh integral (3), an explicit physical interpretation can be given for the stationary position: with a virtual sound field $P(x,y,\omega)$ and a fixed receiver position $\mathbf{x}$, the phase function under consideration is

$$\phi(x_0,\omega) = \phi_{G_{3\mathrm{D}}}(|\mathbf{x}-\mathbf{x}_0|,\omega) + \phi_{P'_y}(\mathbf{x}_0,\omega), \tag{16}$$

where $\phi_{P'_y}(\mathbf{x}_0,\omega)$ denotes the phase of the y-derivative of P taken at $\mathbf{x}_0$, and $\phi_{G_{3\mathrm{D}}}(|\mathbf{x}-\mathbf{x}_0|,\omega)$ denotes the phase of $G_{3\mathrm{D}}(\mathbf{x}-\mathbf{x}_0,\omega)$. The stationary position on the SSD is found where by definition $\phi'(x_0,\omega)=0$ holds, thus

$$\frac{\partial}{\partial x_0}\phi_{G_{3\mathrm{D}}}(|\mathbf{x}_0-\mathbf{x}|,\omega) = -\frac{\partial}{\partial x_0}\phi_{P'_y}(\mathbf{x}_0,\omega). \tag{17}$$

Note, that the reciprocity of the Green's function is used.

A standard prerequisite for the application of the SPA is a rapidly varying phase function compared to the envelope of the oscillation. Thus, when $\phi'_{P,y}(x,y,\omega) \gg \frac{A'_{P,y}(x,y,\omega)}{A_P(x,y,\omega)}$ holds, the derivative of the general polar form (14) can be approximated as

$$\begin{aligned} P'_y(x,y,\omega) &= \left(\frac{A'_{P,y}(x,y,\omega)}{A_P(x,y,\omega)} + \mathrm{j}\phi'_{P,y}(x,y,\omega)\right) P(x,y,\omega) \\ &\approx \mathrm{j}\,\phi'_{P,y}(x,y,\omega)\,P(x,y,\omega). \end{aligned} \tag{18}$$

This expression constitutes the general high-frequency gradient approximation, indicating the local plane wave approximation of an arbitrary sound field.

Due to (18), the phase function of the derivative P'_y in (17) only differs from the phase of P by a constant phase shift. This vanishes due to differentiation and the stationary position for the Rayleigh integral is found where

$$\frac{\partial}{\partial x_0}\phi_{G_{3\mathrm{D}}}(|\mathbf{x}_0-\mathbf{x}|,\omega) = -\frac{\partial}{\partial x_0}\phi_P(x_0,0,\omega) \tag{19}$$

is satisfied.

Hence, the SPA 'compares' the propagation direction/wavefronts ($k_x(x_0)$) of the virtual field and of the Green's function along the SSD. The stationary position is found, where these two directions coincide. See Fig. 1 for an illustration, with the example of a virtual point source. Obviously, by placing back the 3D Green's function at $\mathbf{x}_0$, its wave number vector at $\mathbf{x}$ will coincide with the virtual sound field's wave number vector.

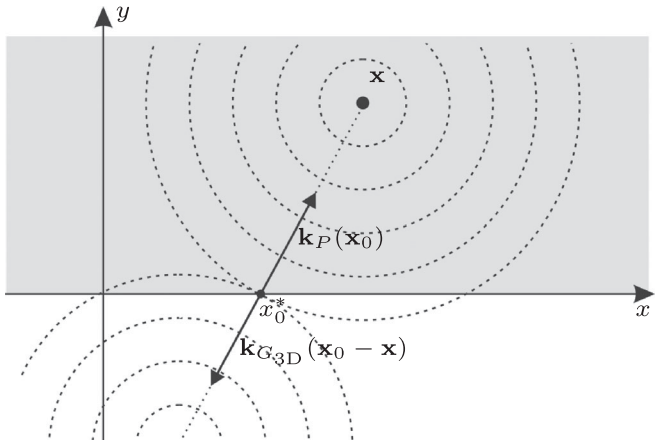

Fig. 1. Geometry for finding the stationary position as the point, where the local propagation direction of the virtual field and a point source at $\mathbf{x}$ coincide.

This result—using the concept of the local wavenumber vector—is of primary importance herein. It states, that for each receiver position $\mathbf{x}$, the synthesized sound field is mostly influenced by that SSD source x_0, from which the emerging spherical wavefronts locally coincide with the target sound field's wavefronts, or in other words the propagation direction of a SSD element and the virtual sound field coincide. And vice versa: every point $\mathbf{x}_0$ on the SSD contributes to the total synthesized sound field mainly along a straight line, pointing from $\mathbf{x}_0$ towards the direction of the wave number vector $\mathbf{k}(\mathbf{x}_0)$ of the target sound field.

For the case of the virtual spherical and the virtual cylindrical wave, this point is found by the intersection of the vector $\mathbf{x}-\mathbf{x}_s$ and the SSD. Although differently derived, this is a well-known result in WFS theory [10, Ch. 3].

B. Unified WFS Driving Functions and Arbitrary Referencing

For the unified WFS formulation we assume a general 3D target sound field, and apply the vertical SPA to its 3D Rayleigh integral representation (3). Assuming an arbitrary non-focused 3D target sound field satisfying $k_z(x, y, 0) = 0$ and fixing the receiver position to the $z = 0$ plane, the vertical stationary point lies trivially at $z^* = 0$. The approximation results in the 2.5D Neumann Rayleigh integral for non-converging / non-focused target fields

$$P(\mathbf{x}, \omega) = -2 \int_{-\infty}^{\infty} \sqrt{\frac{2\pi}{\mathrm{j}\left|\phi''_{P,zz}(\mathbf{x}_0, \omega) + \phi''_{G,zz}(\mathbf{x} - \mathbf{x}_0, \omega)\right|}} \cdot \frac{\partial P(\mathbf{x}, \omega)}{\partial y}\bigg|_{\mathbf{x}=\mathbf{x}_0} G_{3\mathrm{D}}(\mathbf{x} - \mathbf{x}_0), \tag{20}$$

with receiver positions $\mathbf{x} = [x,\ y > 0,\ 0]^{\mathrm{T}}$ and secondary source positions $\mathbf{x}_0 = [x_0,\ 0,\ 0]^{\mathrm{T}}$. It is worth noting that the sign function in (2) reverses for converging/focused sound fields.

As in the foregoing, the 2.5D Rayleigh integral implicitly contains the linear SSD driving functions. We propose the unified WFS driving function

$$D(x_0, \omega) = -\sqrt{\frac{8\pi}{\mathrm{j}k}}\sqrt{d(x_0)}\ \frac{\partial P(\mathbf{x}, \omega)}{\partial y}\bigg|_{\mathbf{x}=\mathbf{x}_0}, \tag{21}$$

with the term $d(x_0)$ denoting the referencing function

$$d(x_0) = \frac{k}{\left|\phi''_{P,zz}(\mathbf{x}_0, \omega) + \phi''_{G,zz}\left(\mathbf{x}(\mathbf{x}_0) - \mathbf{x}_0, \omega\right)\right|}. \tag{22}$$

This function can be chosen in order to reference the synthesis along a prescribed curve, by utilizing the implicit relation $\mathbf{x}(\mathbf{x}_0)$ to be explained. Along this receiver curve positions of amplitude correct synthesis (PCS) exist within the validity of the SPA. The proposed driving function (21) with (22) is a generalization of the revisited WFS (8) and traditional WFS (12) driving function.

The principle of referencing the synthesis originates from the physical interpretation of the horizontal SPA (w.r.t. to x): As each receiver point $\mathbf{x}$ is mainly contributed by one individual SSD element $\mathbf{x}_0$, one may control the amplitude of the synthesized field along an arbitrary convex receiver curve $\mathbf{x}_{\mathrm{ref}}(\mathbf{x}_0)$ by defining the amplitude of the corresponding stationary SSD element $\mathbf{x}_0$ through the referencing function.

Based on the physical interpretation of the SPA, $\mathbf{x}_{\mathrm{ref}}(\mathbf{x}_0)$ is related to $\mathbf{x}_0$ through the implicit relation

$$\mathbf{k}_P(\mathbf{x}_0) = \mathbf{k}_{G_{3\mathrm{D}}}(\mathbf{x}_{\mathrm{ref}}(\mathbf{x}_0) - \mathbf{x}_0). \tag{23}$$

Substituting the explicit expression for the Green's function's wavenumber vector and rearranging leads to

$$\mathbf{x}_{\mathrm{ref}}(x_0) = \mathbf{x}_0 + \frac{\mathbf{k}_P(\mathbf{x}_0)}{k}|\mathbf{x}_{\mathrm{ref}}(\mathbf{x}_0) - \mathbf{x}_0|. \tag{24}$$

The equation is satisfied in radial direction from individual SSD elements along the direction of $\mathbf{k}_P(\mathbf{x}_0)$. As a general statement, the distance at which the individual SSD elements ensure amplitude correct synthesis is given by the amplitude factor of the secondary source dimensionality mismatch $|\mathbf{x}_{\mathrm{ref}}(\mathbf{x}_0) - \mathbf{x}_0|$. This distance is essentially controlled by the referencing function $d(x_0)$.

The PCS are therefore restricted to the parametric reference curve, with the free variable being the SSD position x_0, and the shape of the curve is given by the referencing function and the virtual source model trough $\mathbf{k}_P(x_0)$. In the following it is presented, how the corresponding referencing function $d(x_0)$ may be derived for 2D and 3D virtual sound fields.

C. Referencing 2D Sound Fields

For a 2D target sound field $\phi''_{P,zz}(\mathbf{x}_0, \omega) = 0$ holds and the referencing function (22)

$$d(x_0) = \frac{k}{\left|\phi''_{G,zz}(\mathbf{x}_{\mathrm{ref}}(\mathbf{x}_0) - \mathbf{x}_0, \omega)\right|} = |\mathbf{x}_{\mathrm{ref}}(\mathbf{x}_0) - \mathbf{x}_0| \tag{25}$$

is directly given by the distance of the SSD and the corresponding stationary position along the reference curve. The PCS are given by (cf. (24))

$$\mathbf{x}_{\mathrm{ref}}(x_0) = \begin{bmatrix} x_{\mathrm{ref}}(x_0) \\ y_{\mathrm{ref}}(x_0) \end{bmatrix} = \begin{bmatrix} x_0 + \dfrac{k_x(x_0)}{k}\, d(x_0) \\ \dfrac{k_y(x_0)}{k}\, d(x_0) \end{bmatrix}. \tag{26}$$

As simple examples for 2D virtual sound fields, the virtual plane wave and the virtual line source are investigated.

1) For a Virtual 2D Plane Wave: the wavenumber vector / propagation direction (with $k_z = 0$) is

$$\mathbf{k}_{\mathrm{PW}}(x_0) = \begin{bmatrix} k_x(x_0) \\ k_y(x_0) \end{bmatrix} = k \begin{bmatrix} \cos\varphi_{\mathrm{PW}} \\ \sin\varphi_{\mathrm{PW}} \end{bmatrix} \tag{27}$$

and with (27) inserted into (26) the PCS become

$$\mathbf{x}_{\mathrm{ref,PW}}(x_0) = \begin{bmatrix} x_0 + \cos\varphi_{\mathrm{PW}}\, d(x_0) \\ \sin\varphi_{\mathrm{PW}}\, d(x_0) \end{bmatrix}, \tag{28}$$

illustrated in Fig. 2(a).

2) For a Virtual Line Source: consider a source at $\mathbf{x}_s = [x_s,\ y_s < 0]^{\mathrm{T}}$ with $r_0 = |\mathbf{x}_0 - \mathbf{x}_s|$. For the high-frequency gradient approximation (18), the large argument approximation of the Hankel function [19, (10.2.6)] as the line source model is applied, yielding the local wavenumber vector

$$\mathbf{k}_{\mathrm{LS}}(x_0) = k \begin{bmatrix} \dfrac{x_0 - x_s}{r_0} \\ \dfrac{-y_s}{r_0} \end{bmatrix}. \tag{29}$$

Inserting this into (26) the PCS are

$$\mathbf{x}_{\mathrm{ref,LS}}(x_0) = \begin{bmatrix} x_0 + \dfrac{x_0 - x_s}{r_0}\, d(x_0) \\ \dfrac{-y_s}{r_0}\, d(x_0) \end{bmatrix}. \tag{30}$$

This is also deducible from the geometry in Fig. 2(b).

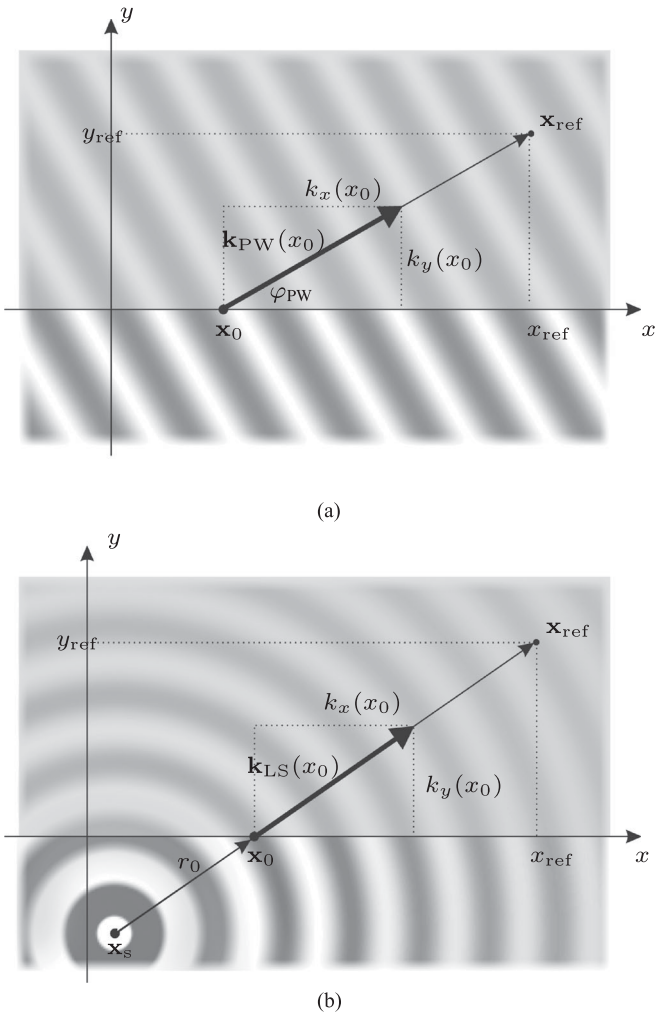

Fig. 2. Geometry for finding the positions of amplitude correct synthesis (PCS) for (a) a plane wave and (b) a line and a point source.

D. Referencing 3D Point Sources

Although the referencing function (22) is valid for an arbitrary 3D sound field, the special case of a virtual point source at position $\mathbf{x}_s = [x_s,\ y_s < 0,\ 0]^{\mathrm{T}}$ with $r_0 = |\mathbf{x}_0 - \mathbf{x}_s|$ is exemplified in the following.

For the point source case the horizontal SPA also holds, and due to the same phase functions in the plane of the synthesis the stationary point remains in the same position in the horizontal direction as for the virtual line source. Again, the synthesis is amplitude correct in a distance of $|\mathbf{x}_{\mathrm{ref}}(\mathbf{x}_0) - \mathbf{x}_0|$ from the stationary SSD element, in radial direction away from the virtual source. Refer to Fig. 2(b) for the geometry.

Substituting the field of the virtual point source into (22), the following referencing function is obtained

$$d(x_0) = \frac{r_0 \cdot |\mathbf{x}_{\mathrm{ref}}(\mathbf{x}_0) - \mathbf{x}_0|}{r_0 + |\mathbf{x}_{\mathrm{ref}}(\mathbf{x}_0) - \mathbf{x}_0|}. \tag{31}$$

Hence, the distance of the PCS measured from the stationary SSD point is

$$|\mathbf{x}_{\mathrm{ref}}(\mathbf{x}_0) - \mathbf{x}_0| = d(x_0)\frac{r_0}{r_0 - d(x_0)}. \tag{32}$$

Comparing the referencing function (25) of virtual 2D sound fields and (32) of the virtual point source, the substitution

$$d(x_0) \rightarrow d(x_0)\frac{r_0}{r_0 - d(x_0)} \tag{33}$$

allows for utilizing the reference curve (30) of the virtual line source. This yields the PCS

$$\mathbf{x}_{\mathrm{ref,PS}}(x_0) = \begin{bmatrix} x_0 + (x_0 & -x_s)\dfrac{d(x_0)}{r_0 - d(x_0)} \\ & -y_s\ \dfrac{d(x_0)}{r_0 - d(x_0)} \end{bmatrix}. \tag{34}$$

More formally the same result is deduced by substituting (32) into (24).

In the following section it is discussed how the referencing function $d(x_0)$ could be chosen in order to reference the synthesized field along a prescribed receiver/reference curve. Furthermore, the analysis allows for the discussion of referencing function's choices in previous WFS approaches.

IV. Application Examples

This section presents application examples for the unified WFS referencing approach via the synthesis of virtual plane waves, line and point sources. The effects of choosing a constant referencing function—as performed in the revisited WFS theory [12], and further simplified in [14]—are investigated. Furthermore, reference curves are exemplarily given for correct synthesis along a line, parallel with the SSD and along a circle around the virtual line/point source, respectively.

All simulations for linear SSDs were carried out by summation of the weighted field of individual 3D secondary point sources at $x_0 = n\,\Delta x_0$ according to

$$P(x, y, \omega) = \sum_{n=-N}^{N} D(x_0, \omega)\, G_{\mathrm{3D}}(x - x_0, y - 0, \omega)\, \Delta x_0, \tag{35}$$

with the sampling distance Δx_0 and total SSD length $2N \cdot \Delta x_0$ chosen such that spatial aliasing and truncation artifacts are negligible. Similarly, for circular SSDs an equiangular spatial sampling scheme for the 3D secondary point sources is deployed. All examples ensure phase correct synthesis within the listening area, therefore only the amplitude deviation is presented in the following. The MATLAB codes, generating all the following simulation examples are available for download,[1] following the reproducible research paradigm.

A. Referencing Schemes for 2D Sound Fields

1) Referencing with Constant d_{ref}: In this referencing scheme the PCS are given by (28) and (30) with a fixed referencing function $d(x_0) = d_{\mathrm{ref}}$ for a plane wave and a line source, respectively. With $d(x_0) = d_{\mathrm{ref}}$ the distance from the stationary SSD element becomes fixed.

As a consequence, a plane wave is referenced along a line parallel to the SSD at $y = \sin\varphi_{\mathrm{PW}}\, d_{\mathrm{ref}}$, whereas the line source

[1] https://github.com/gfirtha/IEEE_unified_WFS

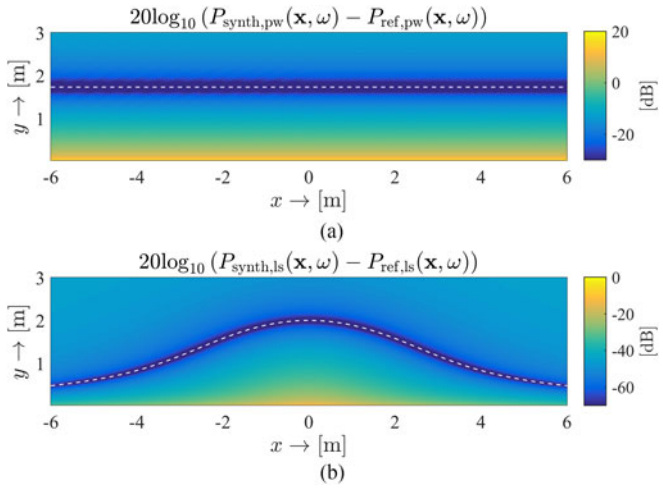

Fig. 3. Constant referencing function. The absolute value of the error measured between the synthesized sound field and the target sound field at $\omega = 2\pi \cdot 1.5\,\text{krad/s}$ for (a) a virtual plane wave with $\varphi_{\text{PW}} = 60°$ and (b) a line source at $\mathbf{x}_s = [0,\ -1]^{\text{T}}$ is shown. The referencing function is set to $d_{\text{ref}} = 2\,\text{m}$. For the virtual plane wave the amplitude is thus referenced along a line at $y = \sin\varphi_{\text{PW}}\, d_{\text{ref}} = 1.73\,\text{m}$. For a virtual line source the positions of amplitude correct synthesis is given by the curve (30) with $d(x_0) \to d_{\text{ref}}$, denoted by the white dashed line. In front of the virtual source the position of amplitude correct synthesis is located at d_{ref}.

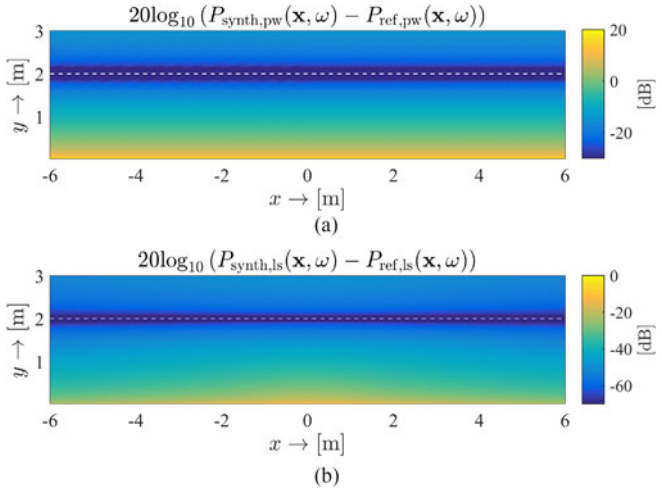

Fig. 4. Referencing along a line, parallel to the SSD. The absolute value of the error measured between the synthesized sound field and the target sound field at $\omega = 2\pi \cdot 1.5\,\text{krad/s}$ for (a) a virtual plane wave with $\varphi_{\text{PW}} = 60°$ and (b) a line source at $\mathbf{x}_s = [0,\ -1]^{\text{T}}$ is shown. The referencing function is set to $d_{\text{line,PW}}(x_0) = 2/\sin\varphi_{\text{PW}}\,\text{m}$ for the plane wave, and $d_{\text{line,LS}}(x_0) = -2r_0/y_s\,\text{m}$ for the line source, resulting in an amplitude correct synthesis at $y_{\text{ref}} = 2\,\text{m}$.

becomes synthesized with correct amplitude along a bell-shaped contour. The maximum distance d_{ref} corresponds directly to the frontal position of the virtual line source. For an illustration see Fig. 3(a) and (b).

2) Referencing along a Parallel Line: With the appropriate choice of $d(x_0)$ in (26) it is possible to reference amplitude correct synthesis along an arbitrary curve. A feasible choice is to reference the synthesis along a line parallel to the SSD at $y = y_{\text{ref}} > 0$. This is achieved by setting the y-entry of the reference curve to a constant value. Hence, cf. (26)

$$d(x_0)_{\text{line,PW,LS}} = \frac{k}{k_y(x_0)}\, y_{\text{ref}}. \tag{36}$$

Referencing functions are obtained via the substitution of the corresponding wavenumber component of a plane wave (27) and a line source (29), respectively. By substituting the resulting $d(x_0)$ back in the WFS driving function (21), the driving functions

$$D_{\text{line,PW}}(x_0, \omega) = +\sqrt{8\pi\,\text{j}\,k_y\, y_{\text{ref}}}\,\text{e}^{-\text{j}k_x x_0}, \tag{37}$$

$$D_{\text{line,LS}}(x_0, \omega) = -\sqrt{\frac{\text{j}\,k\,\pi\, y_{\text{ref}}\, y_s}{2\, r_0}}\, H_1^{(2)}(k r_0) \tag{38}$$

are obtained for the synthesis of a plane wave and a cylindrical wave, respectively. For the case of a virtual plane wave this is precisely equivalent with the Spectral Division Method (SDM) [13, (29)], [14], [21, Ch. 2.4]. The result of the referencing approach is depicted in Fig. 4(a) and (b).

Here it is worthwhile noting that since plane waves constitute an orthogonal basis for arbitrary 2D sound fields, driving functions may be constructed from appropriately referenced plane wave driving functions expressed in terms of k_x and k_y. For the special case of parallel line referencing using (37), the driving function is synthesized by the inverse spatial Fourier transform

$$D(x_0, \omega) = \frac{1}{2\pi}\int_{-\infty}^{\infty} P(k_x, y = 0, \omega)\,\sqrt{8\pi\,\text{j}\,k_y\, y_{\text{ref}}}\,\text{e}^{-\text{j}k_x x_0}\,\text{d}k_x, \tag{39}$$

where $P(k_x, y = 0, \omega)$ denotes the spatio-temporal Fourier spectrum of the virtual sound field evaluated on the SSD.

Alternatively, a corresponding formulation can be given purely in the spatial domain. By expressing the normal derivative in (21) with the high-frequency gradient approximation (18) and substituting the general parallel line referencing function (36), the driving function (21) becomes

$$D(x_0, \omega) = \sqrt{8\pi\,\text{j}\,k_y(x_0)\, y_{\text{ref}}}\, P(x_0, 0, \omega). \tag{40}$$

This formulation requires the pressure and the y-derivative of the phase of the virtual sound field along the SSD.

3) Referencing along a Circle: For a virtual line source it might be feasible in several applications to reference the synthesis along a circle around the center of the virtual source. Consider a circle with a radius of $R_{\text{ref}} > r_0$. From the geometry in Fig. 5 the stationary point $R_{\text{ref}} = d_{\text{ref}} + r_0$ can be deduced, thus

$$d_{\text{circle,LS}}(x_0) = R_{\text{ref}} - r_0. \tag{41}$$

The result of this referencing scheme is shown in Fig. 6.

B. Referencing Schemes for the 3D Point Source

1) Referencing with Constant d_{ref}: The PCS for this case are given by (34) using a constant referencing function $d(x_0) = d_{\text{ref}}$. The resulting reference curve looks similar to that of the line source (cf. Fig. 3(b) vs. Fig. 7(a)), however it exhibits important differences.

The y-coordinate shows a maximum in front of the virtual source, where $r_0 = |y_s|$. For any other y the PCS are closer to

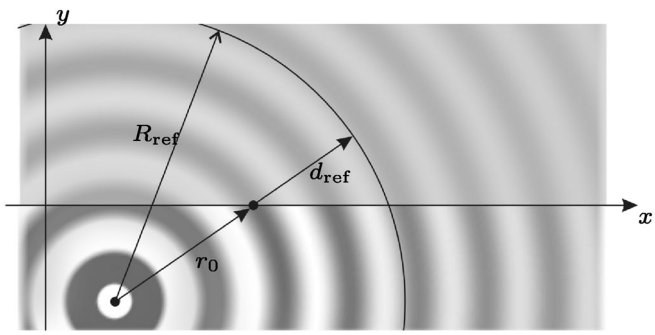

Fig. 5. Geometry for deriving the referencing function along a circle around the virtual line source.

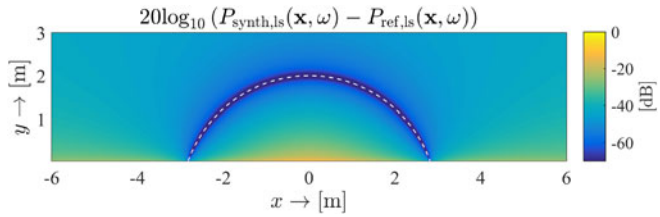

Fig. 6. Referencing a line source along a circle. The absolute value of the error measured between the synthesized sound field and the target sound field for a line source at $\mathbf{x}_s = [0,\ -1]^{\mathrm{T}}$ is shown. The synthesis is referenced on a circle around the line source, with a radius of $R_{\mathrm{ref}} = y_s + 2\,\mathrm{m}$.

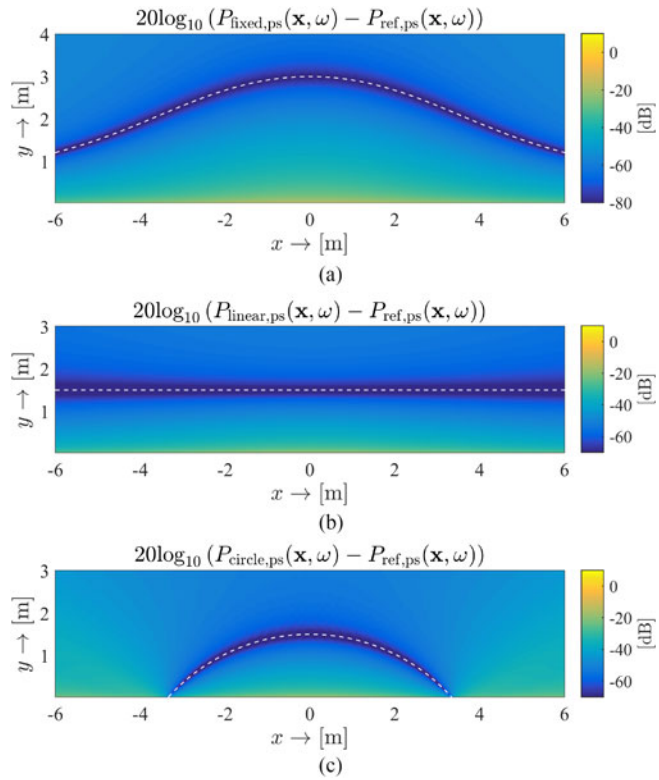

Fig. 7. Referencing the synthesis of a point source (a) with a constant referencing function, (b) to a reference line and (c) to a circle around the virtual source. The virtual source is a point source located at $\mathbf{x}_s = [0,\ -3,\ 0]^{\mathrm{T}}$, oscillating at $\omega = 2\pi \cdot 1.5$ rad/s. For the constant referencing $d_{\mathrm{ref}} = 1.5\,\mathrm{m}$ is set. Note, that in front of the point source the amplitude correct synthesis is ensured at $\frac{y_s}{y_s/d_{\mathrm{ref}}-1} = 3\,\mathrm{m}$. For the case of referencing to a line $y_{\mathrm{ref}} = 1.5\,\mathrm{m}$, while for referencing to a circle $R_{\mathrm{ref}} = y_s + 1.5\,\mathrm{m}$ was chosen.

the SSD. Therefore, $r_0 = |y_s|$ is the critical point of the curve. A position of correct synthesis within the listening area can only be found if $|y_s| > d_{\mathrm{ref}}$. Actually, the synthesis gives a fair result close to the SSD only if $|y_s| \gg d_{\mathrm{ref}}$.

As the virtual source approaches the SSD, the PCS tend to infinity. Here it is stated, that $|y_s|$ should be less than d_{ref}. If d_{ref} is large enough, far field assumptions for the SPA still hold, however no PCS can be found. This type of referencing therefore may suffer from serious amplitude errors in the vicinity of the SSD.

2) Referencing along a Parallel Line: Referencing along a line parallel to the SSD at distance $y = y_{\mathrm{ref}} > 0$ is obtained by fixing the y-entry of (34) to y_{ref}. The referencing function then reads

$$d_{\mathrm{line,PS}}(x_0) = r_0 \frac{y_{\mathrm{ref}}}{y_{\mathrm{ref}} - y_s}. \tag{42}$$

Substituting this back to (21) using the high-frequency gradient approximation of the point source one obtains

$$D(x_0,\omega) = -\sqrt{\frac{\mathrm{j}k}{2\pi}}\sqrt{\frac{y_{\mathrm{ref}}}{y_{\mathrm{ref}} - y_s}}\, y_s \frac{\mathrm{e}^{-\mathrm{j}kr_0}}{r_0^{3/2}}. \tag{43}$$

This result is precisely equivalent with the traditional WFS driving function [11, (2.27)], [10, (3.16)&(3.17)] of a point source, and furthermore identical to the farfield/high-frequency approximated explicit SDM solution [22, (25)], [21, Ch. 2.3]. The result of synthesis by applying this traditional driving function is illustrated in Fig. 7(b).

3) Referencing along a Circle: Referencing the synthesis along a circle around the point source in the synthesis plane is obtained by solving (cf. (33) and (41))

$$d(x_0)\frac{r_0}{r_0 - d(x_0)} = R_{\mathrm{ref}} - r_0, \tag{44}$$

resulting in

$$d_{\mathrm{circle,PS}}(x_0) = r_0 \frac{R_{\mathrm{ref}} - r_0}{R_{\mathrm{ref}}}. \tag{45}$$

The performance of this referencing scheme is demonstrated in Fig. 7(c).

V. Application Examples using Non-Linear Secondary Source Distributions

The general WFS driving functions may be extended for the application of non-linear SSDs [6], [7], [9], [14]. For that the SFS problem can be treated as an equivalent scattering problem. Considering the SSD as the boundary surface of a sound soft scatterer with an incident target sound field of a virtual source, the driving function is obtained by the difference between the normal gradients of the target and the scattered sound field derived on the SSD [7].

A. Kirchhoff Approximation and 2.5D WFS Driving Function

For scattering problems dealing with sound soft boundary surfaces at high frequencies the Kirchhoff approximation [16] is often applied for simplification. The approximation relies on the reflection of plane waves from planar surfaces. If the

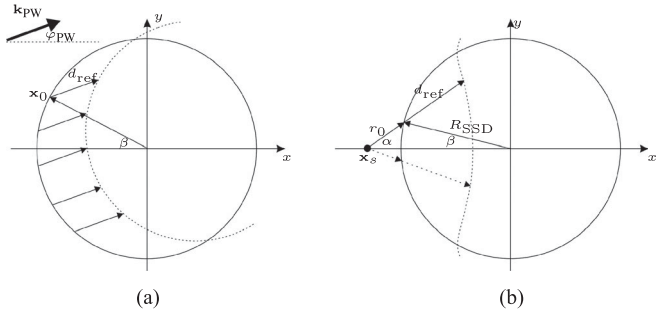

Fig. 8. Geometry for finding the positions of amplitude correct synthesis of (a) a plane wave and (b) a line source.

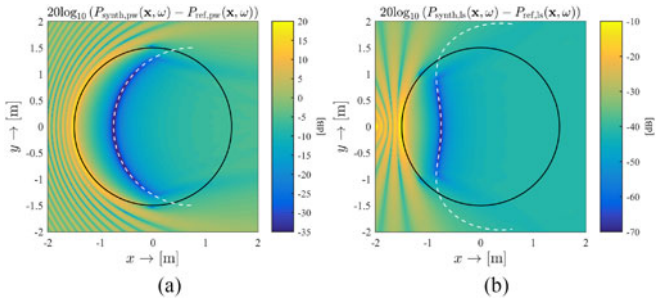

Fig. 9. Positions of amplitude correct synthesis using a circular SSD for (a) a virtual plane wave and (b) a line source. The referencing function is set to $d_{\mathrm{ref}} = 0.75\,\mathrm{m}$. The plane wave propagation direction is set to $\varphi_{\mathrm{PW}} = 0^\circ$ and the virtual line source is located at $\mathbf{x}_s = [-2,\ 0]^{\mathrm{T}}$ with the temporal angular frequency $\omega = 2\pi \cdot 2\,\mathrm{krad/s}$.

reflecting boundary is convex (in order to avoid scattering of the synthesized field) and its dimensions are much larger than the wavelength of the incident target sound field, the surface may be considered locally planar. Then, scattering may be modeled as the reflection of plane waves from planar surfaces. Since the synthesis from arbitrary geometries is thus approximated with that from a planar surface, the general driving function takes the same form as the driving function using a planar SSD. The same concept holds for 2.5D SFS deploying curved SSD contours. For practical importance we restrict the discussion to this case in the followings.

However, only those SSD elements contribute to the synthesis, that are 'illuminated' by the incident sound field, i.e. whose sound field propagates into the same direction as the target sound field within the synthesis plane. This requirement is formulated with the spatial windowing function $w(\mathbf{x}_0)$

$$w(\mathbf{x}_0) = \begin{cases} 1 & \text{if} \quad \langle \mathbf{k}(\mathbf{x}_0), \mathbf{n}_i(\mathbf{x}_0) \rangle > 0 \\ 0 & \text{elsewhere,} \end{cases} \tag{46}$$

where $\mathbf{k}(\mathbf{x}_0)$ denotes the local wavenumber vector as defined in the foregoing and $\mathbf{n}_i(\mathbf{x}_0)$ being the unit inward normal of the SSD. In the context of WFS this windowing is referred to as the secondary source selection [23], [24].

With all these approximations the unified 2.5D WFS driving function for a curved SSD contour reads, cf. (21)

$$D(\mathbf{x}_0, \omega) = -w(\mathbf{x}_0) \sqrt{\frac{8\pi}{\mathrm{j}k}} \sqrt{d(\mathbf{x}_0)}\, \frac{\partial P(\mathbf{x}, \omega)}{\partial \mathbf{n}_i}\bigg|_{\mathbf{x}=\mathbf{x}_0}. \tag{47}$$

In the following it is demonstrated, that the referencing approach, described above can be applied without modification to arbitrary SSD contours. Since both, the SPA and the Kirchhoff approximation are valid for high frequencies, no further presumptions are required.

B. Referencing Schemes for a Circular SSD

The validity of the referencing schemes is demonstrated via the example of a circular SSD in the $x-y$-plane with radius R_{SSD} centered around the origin. For this SSD type the normal derivative is given by the radial derivative. The WFS driving function as well as the referencing function only depend on the polar angle β, cf. Fig. 8.

The referencing function $d(\beta)$ for an arbitrary reference curve can be found in the same manner as for the linear SSD using the SPA. Here, geometrical considerations lead to a convenient derivation. As stated before, the stationary secondary source can be found where the wavenumber vector intersects the SSD. This is the constant vector $\mathbf{k}_{\mathrm{PW}}$ for a plane wave and any radial vector from the source position for the line and the point source. In the following, referencing the synthesis along a straight line and along a concentric circle inside the circular SSD are discussed.

1) Referencing with Constant d_{ref}: First, the effect of a constant referencing function is investigated. For both, the plane wave and the line source, the PCS can directly be deduced from the problem's geometry.

For the plane wave case, the points from each SSD element at a distance of d_{ref} describe a circle with radius R_{SSD}, translated into the wave propagating direction by d_{ref}, cf. Fig. 8(a). The PCS are therefore given by

$$\mathbf{x}_{\mathrm{ref,PW}}(\mathbf{x}_0) = \begin{bmatrix} \cos\beta\, R_{\mathrm{SSD}} + \cos\varphi_{\mathrm{PW}}\, d_{\mathrm{ref}} \\ \sin\beta\, R_{\mathrm{SSD}} + \sin\varphi_{\mathrm{PW}}\, d_{\mathrm{ref}} \end{bmatrix}. \tag{48}$$

For a virtual line source, cf. Fig. 8(b), the reference curve can be deduced to

$$\mathbf{x}_{\mathrm{ref,LS}}(\mathbf{x}_0) = \begin{bmatrix} x_s + \cos\alpha\,(d_{\mathrm{ref}} + r_0) \\ y_s + \sin\alpha\,(d_{\mathrm{ref}} + r_0) \end{bmatrix}. \tag{49}$$

This curve is not easily accessible for analytic investigation, however two limiting cases are apparent. As the virtual source approaches the SSD, the curve describes a circle around the virtual source with the radius d_{ref}. If the virtual source is very far from the SSD the incident field becomes a plane wave. As discussed above, the curve then describes a circle with a radius R_{SSD} translated by d_{ref} into the direction defined by the position vector of the virtual source. It is also ensured, that in front of the virtual source, the distance of amplitude correct synthesis from the corresponding SSD element is d_{ref}. Results of numeric simulations, using these referencing schemes are depicted in Fig. 9.

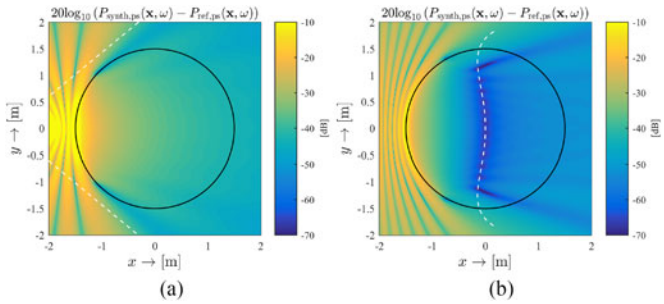

Fig. 10. Positions of amplitude correct synthesis using a circular SSD with radius of $R_{\mathrm{SSD}} = 1.5\,\mathrm{m}$ for a virtual point source with the virtual source positioned at (a) $\mathbf{x}_s = [-2,\ 0,\ 0]^{\mathrm{T}}$ and (b) $\mathbf{x}_s = [-3,\ 0,\ 0]^{\mathrm{T}}$ oscillating at $\omega = 2\pi \cdot 2\,\mathrm{krad/s}$. The referencing function is set to $d_{\mathrm{ref}} = 0.75\,\mathrm{m}$. In (a) $r_0 < d_{\mathrm{ref}}$, therefore no position for correct synthesis can be found. As the virtual source gets further from the SSD (b), $r_0 > d_{\mathrm{ref}}$ is satisfied, and the position of correct synthesis in front of the virtual source becomes $x_c = x_s + r_0 \frac{r_0}{r_0 - d_{\mathrm{ref}}} = 0$.

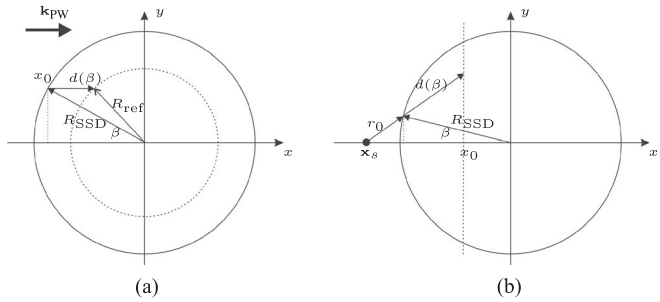

Fig. 11. Geometry for finding $d(\varphi)$ referencing the synthesis of a plane wave to a concentric circle (a) and the synthesis of a line source to a straight line (b).

For the synthesis of a virtual point source the mapping (33) is applied to (49). The PSC are then given as

$$\mathbf{x}_{\mathrm{ref,PS}}(\mathbf{x}_0) = \begin{bmatrix} x_s + \cos\alpha\, r_0 \dfrac{r_0}{r_0 - d} \\ y_s + \sin\alpha\, r_0 \dfrac{r_0}{r_0 - d} \end{bmatrix}. \tag{50}$$

Numerical simulations are visualized in Fig. 10. Similarly to the linear SSD case, no PCS can be found if the point source is closer to the SSD than the reference distance. This can be observed in Fig. 10(a).

2) Referencing to an Arbitrary Curve: Finally, arbitrary reference curves for circular SSD contours are discussed. For that referencing a plane wave along a circle and—due to practical importance—referencing a point source along a line are exemplarily chosen, cf. the geometries in Fig. 11. The referencing function $d(\beta)$, equaling the length of the corresponding vector can be derived with geometrical considerations to

$$d_{\mathrm{circle,PW}}(\beta) = R_{\mathrm{SSD}} \cos\beta - \sqrt{R_{\mathrm{ref}}^2 - R_{\mathrm{SSD}}^2 \sin^2\beta}, \tag{51}$$

$$d_{\mathrm{line,LS}}(\beta) = -r_0 \left(\frac{x_0 + R_{\mathrm{SSD}} \cos\beta}{x_s + R_{\mathrm{SSD}} \cos\beta} \right), \tag{52}$$

$$d_{\mathrm{line,PS}}(\beta) = r_0 \frac{x_0 + R_{\mathrm{SSD}} \cos\beta}{x_0 - x_s}. \tag{53}$$

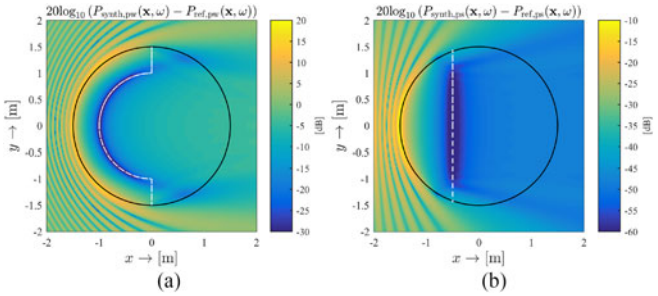

Fig. 12. Result of referencing the synthesis of (a) a plane wave to a circle and (b) a point source to a line. The source frequency was set to $\omega_0 = 2\pi \cdot 2\,\mathrm{krad/s}$, the plane wave propagates parallel to the x-axis ($\varphi_{\mathrm{PW}} = 0$) and the point source is located at $\mathbf{x}_s = [-3,\ 0,\ 0]^{\mathrm{T}}$. The radius of the reference circle is $R_{\mathrm{ref}} = 1\,\mathrm{m}$ at (a) and the line of referencing is located at $x_0 = -1.25\,\mathrm{m}$ in (b).

The latter was again derived from $d_{\mathrm{line,LS}}(\beta)$ with the mapping (33). Numerical simulations for the referencing functions $d_{\mathrm{circle,PW}}(\beta)$ and $d_{\mathrm{line,PS}}(\beta)$ prove the concept and are shown in Fig. 12.

VI. Conclusion

Unified 2.5D Wave Field Synthesis (WFS) driving functions were proposed, allowing the optimization of the amplitude distribution of synthesized 2D or 3D sound fields to various reference curves. The backbone of 2.5D WFS is formed by the stationary phase approximation (SPA). It is discussed, that the SPA explicitly finds the stationary point along the secondary source distribution (SSD), where its emitted wavefront coincides with the virtual sound field's wavefront in an arbitrary receiver position. This interpretation of the SPA is formalized via the introduction of the local wavenumber vector concept. By individually controlling the SSD elements' amplitude factor in the stationary position, synthesis can be optimized along arbitrary receiver curves for linear and curved SSD contours. Compared to previous WFS approaches, novel and improved referencing schemes for both linear and circular SSDs are derived that can be directly implemented for practical setups.

Well-known WFS referencing schemes are revisited by investigating the region of their validity in an analytical manner. It is verified, that using a constant and 'target sound field'-independent referencing function, the synthesis of 2D sound fields is feasible and well-behaved. For the case of a 3D virtual sound field, e.g. a point source, a virtual source dimensional mismatch appears besides the well-studied secondary source dimensionality mismatch. Unless a compensation term is introduced to the amplitude factor—resulting in the traditional 2.5D WFS driving functions for a linear SSD with a parallel receiving curve—the positions of amplitude correct synthesis highly depend on the virtual source position. For sources close to the SSD this may cause large amplitude deviations. In order to compensate the occurring amplitude error, one should include the amplitude correction factor, when a 3D field is to be synthesized. If alternatively a constant referencing function is preferred, applying 2D virtual source models should be considered.

Besides the theoretical results the presented framework includes a number of practical application possibilities. In the

foregoing simple sound scenes were investigated with only one plane wave component or a single point source. When complex sound scenes are considered only the choice of a reference line and of a reference circle will ensure amplitude correct synthesis along the reference curve for a linear and circular SSD, respectively. These referencing approaches for arbitrary target fields are made possible in the present treatise for the first time. Furthermore, the presented framework allows the optimization of amplitude correct reproduction for applications with known audience area geometries, e.g. in case of large-scale sound reinforcement using line source arrays in concert venues [25].

REFERENCES

[1] A. Berkhout, "A holographic approach to acoustic control," *J. Audio Eng. Soc.*, vol. 36, no. 12, pp. 977–995, 1988.

[2] A. J. Berkhout, D. de Vries, and P. Vogel, "Acoustic control by wave field synthesis," *J. Acoust. Soc. Amer.*, vol. 93, no. 5, pp. 2764–2778, 1993.

[3] P. Vogel, "Application of wave field synthesis in room acoustics," Ph.D. dissertation, Faculty Appl. Physics, Delft Univ. Technol., Delft, The Netherlands, 1993.

[4] D. de Vries, *Wave Field Synthesis—AES Monograph*. New York, NY, USA: Audio Engineering Soc., 2009.

[5] S. Spors, H. Wierstorf, A. Raake, F. Melchior, M. Frank, and F. Zotter, "Spatial sound with loudspeakers and its perception: A review of the current state," *Proc. IEEE*, vol. 101, no. 9, pp. 1920–1938, Sep. 2013.

[6] F. Zotter and S. Spors, "Is sound field control determined at all frequencies? How it is related to numerical acoustics?" in *Proc. 52nd Audio Eng. Soc. Intl. Conf.*, Guildford, U.K., Sep. 2013, Paper no. 1–3.

[7] F. Fazi and P. Nelson, "Sound field reproduction as an equivalent acoustical scattering problem," *J. Acoust. Soc. Amer.*, vol. 134, no. 5, pp. 3721–3729, 2013.

[8] D. de Vries, "Sound reinforcement by wavefield synthesis: Adaptation of the synthesis operator to the loudspeaker directivity characteristics," *J. Audio Eng. Soc.*, vol. 44, no. 12, pp. 1120–1131, 1996.

[9] E. W. Start, "Application of curved arrays in wave field synthesis," in *Proc. 100th Audio Eng. Soc. Conv.*, Copenhagen, Denmark, May 1996, pp. 1–23, Paper no. 4143.

[10] E. Start, "Direct sound enhancement by wave field synthesis," Ph.D. dissertation, Faculty Appl. Physics, Delft Univ. Technol., Delft, The Netherlands, 1997.

[11] E. Verheijen, "Sound reproduction by wave field synthesis," Ph.D. dissertation, Faculty Appl. Physics, Delft Univ. Technol., Delft, The Netherlands, 1997.

[12] S. Spors, R. Rabenstein, and J. Ahrens, "The theory of wave field synthesis revisited," in *Proc. 124th Audio Eng. Soc. Conv.*, Amsterdam, The Netherlands, May 2008, pp. 1–19, Paper no. 7358.

[13] J. Ahrens and S. Spors, "Sound field reproduction using planar and linear arrays of loudspeakers," *IEEE Trans. Audio, Speech, Lang. Process.*, vol. 18, no. 8, pp. 2038–2050, Nov. 2010.

[14] J. Ahrens, *Analytic Methods of Sound Field Synthesis*. Berlin, Germany: Springer, 2012.

[15] N. Bleistein, *Mathematical Methods for Wave Phenomena*. Orlando, FL, USA: Academic, 1984.

[16] N. Bleistein and R. Handelsman, *Asymptotic Expansions of Integrals*. New York, NY, USA: Dover, 1986.

[17] E. G. Williams, *Fourier Acoustics*, 1st ed. London, U.K.: Academic, 1999.

[18] E. Skudrzyk, *The Foundations of Acoustics*. New York, NY, USA: Springer, 1971.

[19] F. W. J. Olver, D. W. Lozier, R. F. Boisvert, and C. W. Clark, *NIST Handbook of Mathematical Functions*, 1st ed. Cambridge, U.K.: Cambridge Univ. Press, 2010.

[20] F. Völk and H. Fastl, "Wave Field Synthesis with primary source correction: Theory, simulation results, and comparison to earlier approaches," in *Proc. 133rd Audio Eng. Soc. Conv.*, San Francisco, CA, USA, Oct. 2012, pp. 1–20, Paper no. 8717.

[21] F. Schultz, "Sound field synthesis for line source array applications in large-scale sound reinforcement," Ph.D. dissertation, Faculty Comput. Sci. Elect. Eng., Univ. Rostock, Rostock, Germany, 2016.

[22] S. Spors and J. Ahrens, "Analysis and improvement of pre-equalization in 2.5-dimensional wave field synthesis," in *Proc. 128th Audio Eng. Soc. Conv.*, London, U.K., May 2010, pp. 1–17, Paper no. 8121.

[23] R. Nicol and M. Emerit, "3D-sound reproduction over an extensive listening area: A hybrid method derived from holophony and ambisonic," in *Proc. 16th Audio Eng. Soc. Intl. Conf.*, Rovaniemi, Finland, Apr. 1999, pp. 436–453, Paper no. 16-039.

[24] S. Spors, "Extension of an analytic secondary source selection criterion for wave field synthesis," in *Proc. 123rd Audio Eng. Soc. Conv.*, New York, NY, USA, Oct. 2007, pp. 1–15, Paper no. 7299.

[25] F. Schultz, G. Firtha, P. Fiala, and S. Spors, "Wave field synthesis driving functions for large-scale sound reinforcement using line source arrays," in *Proc. 142nd Audio Eng. Soc. Conv.*, Berlin, Germany, May 2017, pp. 1–14, Paper no. 9722.

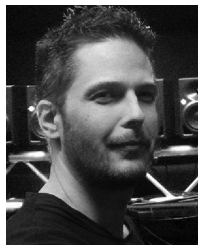

Gergely Firtha was born in Budapest, Hungary, in 1986. He received the B.S. and M.S degrees from Budapest University of Technology and Economics, Budapest, Hungary, in 2009 and 2011, respectively. He is currently a Research Assistant in the Laboratory of Acoustics and Studio Technics, Department of Networked Systems and Services. His main research interests include acoustic signal processing and multichannel sound field reproduction.

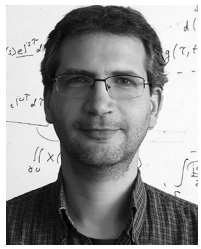

Péter Fiala was born in Budapest, Hungary, in 1978. He received the Ph.D. degree in electrical engineering from Budapest University of Technology and Economics, Budapest, Hungary, in 2009. He is currently working as an Assistant Professor in the Department of Networked Systems and Services. His main research interests include the field of computational acoustics, acoustic signal processing and noise and vibration control.

Frank Schultz received the M.Sc. degree in audio communication and technology from Technische Universität Berlin, Berlin, Germany, and the Dr.-Ing. degree with distinction from the Universität Rostock, Rostock, Germany, in 2011 and 2016, respectively. His current research interests include sound field synthesis applications and signal processing for loudspeaker arrays. He is a Visiting Postdoc in the Audio Communication Group, Technische Universität Berlin. He is a member of the Audio Engineering Society (AES) and reviews for the AES and the IEEE.

Sascha Spors (M'11) received the Dipl.-Ing. degree in electrical engineering and the Dr.-Ing. degree with distinction from the University of Erlangen-Nuremberg, Erlangen, Germany, in 2000 and 2006, respectively.

He is currently the head of the Virtual Acoustics and Signal Processing Group as a Professor, Institute of Telecommunications Engineering, Universität Rostock, Rostock, Germany. From 2005 to 2012, he was heading the Audio Technology Group as a Senior Research Scientist, Telekom Innovation Laboratories, Technische Universität Berlin, Berlin, Germany. From 2001 to 2005, he was a member of the Research Staff at the Chair of Multimedia Communications and Signal Processing, University of Erlangen-Nuremberg. He holds several patents, and has authored or coauthored several book chapters and more than 200 papers in journals and conference proceedings. His current research interests include sound field analysis and reproduction using multichannel techniques, the perception of synthetic sound fields, and open science. He is a member of the Audio Engineering Society (AES) and the German Acoustical Society. He was awarded the Board of Governors Award of the Audio Engineering Society in 2015 and the Lothar Cremer prize of the German Acoustical Society in 2011. He is a Co-Chair of the AES Technical Committee on Spatial Audio and an Associate Technical Editor of the Journal of the Audio Engineering Society and the IEEE SIGNAL PROCESSING LETTERS.